Journal of Solid State Chemistry 183 (2010) 2570–2575

Contents lists available at ScienceDirect

Journal of Solid State Chemistry

journal homepage: www.elsevier.com/locate/jssc

Synthesis and structural characterization of a new aluminum oxycarbonitride, $Al_5(O, C, N)_4$

Haruya Inuzuka [a], Motoaki Kaga [a], Daisuke Urushihara [a], Hiromi Nakano [b], Toru Asaka [a], Koichiro Fukuda [a,*]

[a] Department of Environmental and Materials Engineering, Nagoya Institute of Technology, Nagoya 466-8555, Japan
[b] Cooperative Research Facility Center, Toyohashi University of Technology, Toyohashi 441-8580, Japan

ARTICLE INFO

Article history:
Received 1 June 2010
Received in revised form
30 August 2010
Accepted 31 August 2010
Available online 8 September 2010

Keywords:
Crystal structure
Powder diffraction
Rietveld method
New material
Aluminum oxycarbonitride
Al_5C_3N

ABSTRACT

A new aluminum oxycarbonitride, $Al_5(O_xC_yN_{4-x-y})$ ($x\sim1.4$ and $y\sim2.1$), has been synthesized and characterized by X-ray powder diffraction, transmission electron microscopy and electron energy loss spectroscopy (EELS). The title compound was found to be hexagonal with space group $P6_3/mmc$, $Z=2$, and unit-cell dimensions $a=0.328455(6)$ nm, $c=2.15998(3)$ nm and $V=0.201805(6)$ nm^3. The atom ratios O:C:N were determined by EELS. The final structural model, which is isomorphous with that of $(Al_{4.4}Si_{0.6})(O_{1.0}C_{3.0})$, showed the positional disordering of one of the three types of Al sites. The maximum-entropy method-based pattern fitting (MPF) method was used to confirm the validity of the split-atom model, in which conventional structure bias caused by assuming intensity partitioning was minimized. The reliability indices calculated from the MPF were $R_{wp}=6.94\%$ ($S=1.22$), $R_p=5.34\%$, $R_B=1.35\%$ and $R_F=0.76\%$. The crystal was an inversion twin. Each twin-related individual was isostructural with Al_5C_3N (space group $P6_3mc$, $Z=2$).

1. Introduction

A series of ternary carbonitrides in the Al_4C_3–AlN system [1,2] can be represented by a general formula $Al_4C_3(AlN)_X$, where $X=1$ (Al_5C_3N), 2 ($Al_6C_3N_2$), 3 ($Al_7C_3N_3$) and 4 ($A1_8C_3N_4$). These carbonitrides have the characteristics of layered structures consisting of two types of layers. One is an $[Al_4(C, N)_4]$ unit layer (A), which is composed of an $[Al_2(C, N)_2]$ double layer of $Al(C, N)_4$ tetrahedra surrounded by two $[Al(C, N)_2]$ single layers of $Al(C, N)_4$ tetrahedra. The other is an $[Al(C, N)_2]$ single layer (B) of $Al(C, N)_4$ tetrahedra. The structure of Al_5C_3N (space group $P6_3mc$, $Z=2$) is build up of alternately stacking two types of layers with the sequence of $\langle BABA\rangle$. For the rhombohedral lattice of $Al_6C_3N_2$ ($R\bar{3}\,m$, $Z=3$), the stacking sequence is $\langle BABBABBAB\rangle$. The crystal structures of the other aluminum carbonitrides are also made up of the combinations of A and B layers with the stacking sequences of $\langle BBABBBAB\rangle$ for $Al_7C_3N_3$ (space group $P6_3mc$, $Z=2$) and $\langle BBABBBBABBBBABB\rangle$ for $A1_8C_3N_4$ ($R\bar{3}m$, $Z=3$).

In the system Al–Si–O–C, the authors have discovered and structurally characterized two types of new aluminum silicon oxycarbides; $(Al_{18-x}Si_x)(O_yC_{14-y})$ ($x\sim1.2$ and $y\sim3.0$) and $(Al_{5-x}Si_x)(O_yC_{4-y})$ ($x\sim0.6$ and $y\sim1.0$) [3,4]. Each of these crystals has been found to be made up of two domains, which are related by pseudo-symmetry inversion. The dimensions of twin domains were within the coherence range of X-rays and the domain ratios were 0.5:0.5 for both compounds, hence the crystal structures have been successfully represented by the split-atom models. These compounds are characterized by the crystal structures consisting of the A-type $[(Al, Si)_4(O, C)_4]$ unit layer and B-type $[(Al, Si)(O, C)_2]$ single layer. The monoclinic structure of $(Al_{16.8}Si_{1.2})(O_{3.0}C_{11.0})$ (space group $C2/m$, $Z=1$) is build up of these layers with the stacking sequence of $\langle ABA\rangle$. For the hexagonal lattice of $(Al_{4.4}Si_{0.6})(O_{1.0}C_{3.0})$ ($P6_3/mmc$, $Z=2$), the stacking sequence is $\langle ABAB\rangle$ and/or $\langle BABA\rangle$.

Recent advances in the field of crystal-structure analysis from X-ray powder diffraction (XRPD) data have enabled us to investigate disordered crystal structures. The structural parameters are usually refined using the Rietveld method [5]. A combined use of the Rietveld method, the maximum-entropy method (MEM) [6] and the MEM-based pattern fitting (MPF) method [7] has enabled us to disclose new structural details. MEM is capable of estimating structure factors of unobserved reflections and improving those of overlapped reflections, which give MEM advantages over the classical Fourier method. However, the Rietveld method and MEM have a drawback in determining the electron-density distributions (EDD) because the observed structure factors, F_o(Rietveld), are biased toward the structural model adopted in Rietveld analysis. On the other hand, the MPF method can minimize the structural bias. Thus, MEM analysis and whole-pattern fitting are alternately repeated (REMEDY cycle)

* Corresponding author. Fax: +81 52 735 5289
E-mail address: fukuda.koichiro@nitech.ac.jp (K. Fukuda).

0022-4596/$ - see front matter © 2010 Elsevier Inc. All rights reserved.
doi:10.1016/j.jssc.2010.08.043

until the reliability indices reach minima. Crystal structures can be seen clearly from EDD determined by MPF.

In the present study, we have discovered a new aluminum oxycarbonitride in the Al–O–C–N system. The crystal structure was isostructural with $(Al_{5-x}Si_x)(O_yC_{4-y})$ ($x\sim0.6$ and $y\sim1.0$). We used the MPF method to confirm the validity of the split-atom model, in which one of the three types of Al sites was positionally disordered. The crystal was most probably an inversion twin with nearly the same twin fraction.

2. Experimental

2.1. Synthesis

The reagent-grade chemicals of AlN (99.9%, KCL Co., Ltd, Saitama, Japan) and Al_4C_3 (98%, Mitsuwa Chemical Co., Ltd, Kanagawa, Japan) were mixed in molar ratios of $AlN:Al_4C_3=1:1.5$. The well-mixed chemicals were pressed into pellets (ϕ15 mm × 10 mm), loaded into an open carbon crucible, heated in a carbon resistance furnace at 2173 K for 1 h in inert gas atmosphere of Ar, followed by cooling to ambient temperature by cutting furnace power. The Ar gas that was flowing in the furnace contained a very small amount of O_2 gas. Thus, the experimental oxygen partial pressure (P_{O_2}) was most probably near the carbon–carbon monoxide (CCO) buffer. The P_{O_2}-value at 2173 K was estimated to be 8.9×10^{-15} atm ($\log P_{O_2}=-14.05$) based on the CCO buffer (Fig. 1) [8]. The procedures of mixing and heating were repeated twice for complete homogenization. The reaction product was a slightly sintered polycrystalline material.

2.2. Characterization

The sample was finely ground to obtain powder specimen. A diffractometer (X'Pert PRO Alpha-1, PANalytical B.V., Almelo, the Netherlands), equipped with an incident-beam Ge(111) Johansson monochromator to obtain Cu$K\alpha_1$ radiation and a high-speed detector, was used in the Bragg–Brentano geometry. The X-ray generator was operated at 45 kV and 40 mA. An automatic divergence slit was used to keep a constant illuminated length of 5 mm on the specimen surface. Other experimental conditions were: continuous scan, experimental 2θ range from 5.0012° to 148.9186° (an accuracy in 2θ of $\pm0.0001°$), 17 225 total data points and 6.5 h total experimental time. The entire experimental diffraction pattern was employed for the crystal-structure analysis. Structural parameters were refined by the Rietveld method using the computer program RIETAN-FP [9]. The crystal-structure models and equidensity isosurfaces of EDD were visualized with the computer program VESTA [10].

The powder specimen was also examined using a transmission electron microscope (JEM 2100F, JEOL Ltd., Tokyo, Japan) operated at 200 kV and equipped with an electron energy loss spectrometer (Enfina, Gatan Inc., Pleasanton, CA, USA). The powder particles were deposited with ethyl alcohol on a copper grid. Selected area electron diffraction (SAED) patterns and corresponding lattice images were obtained.

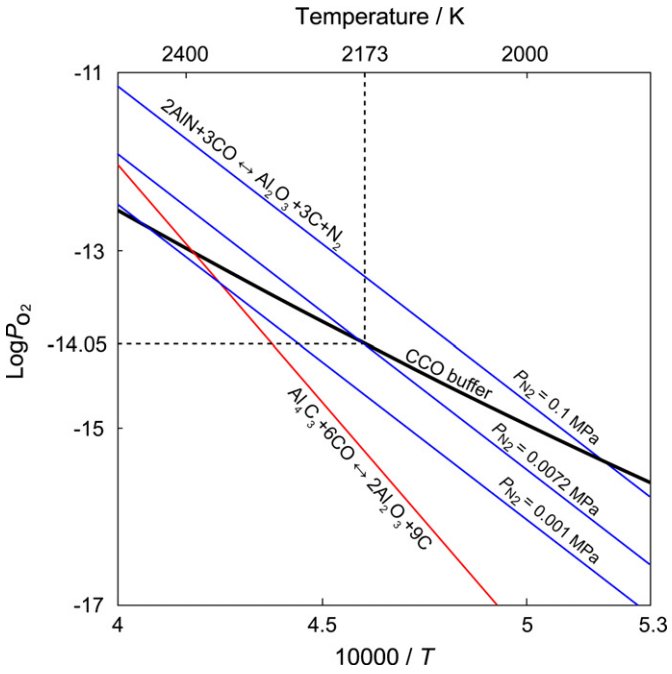

Fig. 1. Comparison of phase boundaries in the systems C–O, Al–O–C and Al–O–C–N as a function of temperature and oxygen partial pressure. The thick curve of carbon–carbon monoxide (CCO) buffer is from [8]. The curves of phase boundaries for Al_4C_3 (s)+6CO (g)↔2Al_2O_3 (s)+9C (s) and AlN (s)+3CO (g)↔Al_2O_3 (s)+3C (s)+N_2 (g) are calculated using data from [17]. Because the latter boundary is dependent on the partial pressure of N_2 (P_{N_2}), the three types of boundary lines are depicted for $P_{N_2}=0.1$, 0.0072 and 0.001 MPa.

3. Results and discussion

3.1. Chemical composition and structure refinement

The SAED pattern was successfully indexed with a hexagonal unit cell with dimensions of $a\approx0.33$ nm and $c\approx2.2$ nm (Fig. 2). The corresponding lattice image strongly suggests that the crystal is characterized by a layered structure with the periodicity of about 2.2 nm along the c-axis. The electron energy loss spectrum (EELS) showed the existence of O, C and N atoms (Fig. 3). The O atoms, together with C and N atoms, are most probably located within the crystal lattice, not concentrated on the crystal grain surface. The O atoms might be originated from the impurities of AlN as well as Ar gas and introduced into the sample during the crystal growth process. The atom ratios O:C:N were determined from EELS to be 0.34(10):0.52:0.14(4), where the numbers in parentheses indicate measurement error.

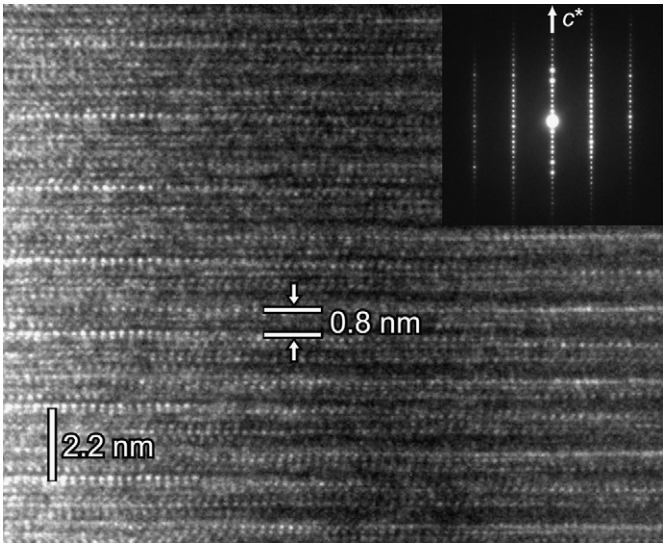

Fig. 2. Selected-area electron diffraction pattern and corresponding lattice image. Incident beam almost parallel to the a-axis. The lattice image shows mutually interpenetrating twin-related domains. The fringes around the domain boundary show translational misfit of approximately 0.8 nm along the c direction.

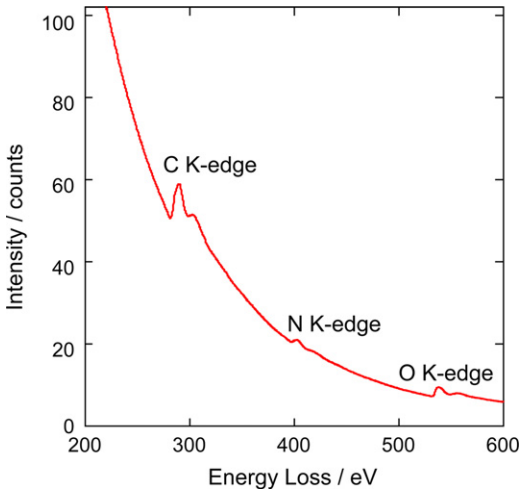

Fig. 3. Identification of the presence of O, C and N in the compound. Electron energy loss spectrum.

Table 1
Crystal data for $Al_5(O_{1.4}C_{2.1}N_{0.5})$.

Chemical composition	$Al_5O_{1.4}C_{2.1}N_{0.5}$
Space group	$P6_3/mmc$
a (nm)	0.328455(6)
c (nm)	2.15998(3)
V (nm^3)	0.201805(6)
Z	2
D_x (Mg m^{-3})	3.12

The XRPD pattern showed the presence of very weak diffraction intensities peculiar to Al_4C_3; hence the unit-cell parameters as well as the integrated intensities of the new compound were refined by the Le Bail method [11] using the computer program RIETAN-FP. The refined unit-cell dimensions were $a=0.328489(5)$ nm and $c=2.15983(2)$, which could successfully index all the observed reflections in the experimental diffraction pattern. The intensity distributions of XRPD pattern as well as the refined unit-cell dimensions were compatible with those of $(Al_{4.4}Si_{0.6})(O_{1.0}C_{3.0})$ [4]. Thus, this compound is most probably isostructural with $(Al_{4.4}Si_{0.6})(O_{1.0}C_{3.0})$, the unit-cell content of which is [10Al 2.8O 4.2C 1.0N].

Initial structural parameters of $Al_5(O_{1.4}C_{2.1}N_{0.5})$ ($Z=2$) were taken from those determined by Kaga et al. [4] for $(Al_{4.4}Si_{0.6})(O_{1.0}C_{3.0})$. There are six independent sites in the structural model; three Al sites are located at the Wyckoff positions 4*e* (Al1) and 4*f* (Al2 and Al3), and three (O, C, N) sites are located at 2*a*, 2*b* and 4*f*. The structural model is characterized by the split site for Al3, the site occupancy of which is 1/2. The atomic scattering factors used were calculated from the coefficients for their analytical approximations for neutral Al, O, C and N. The structural parameters were refined by the Rietveld method using the computer program RIETAN-FP. The structure model of Al_4C_3 [12] was added into the refinement as an additional phase. A Legendre polynomial was fitted to background intensities with 12 adjustable parameters. The split Pearson VII function [13] was used to fit the peak profile. The isotropic atomic displacement parameters (B) of the (O, C, N) sites were constrained to have the same value. The reliability indices [14] for the final result were $R_{wp}=7.25\%$, $S=1.27$ and $R_p=5.58\%$ ($R_B=3.32\%$ and $R_F=1.89\%$ for $Al_5(O_{1.4}C_{2.1}N_{0.5})$). Crystal data are given in Table 1, and the final atomic positional and B parameters are given in Table 2. Quantitative X-ray analysis with correction for microabsorption according to Brindley's procedure [15] was implemented in the program RIETAN-FP. The phase composition of the sample was found to be 95.9 mol% $Al_5(O_{1.4}C_{2.1}N_{0.5})$ and 4.1 mol% Al_4C_3, on the assumption that both effective particle radii of the two phases were 5.00 μm. Fig. 4 shows the final structural model, which has been confirmed to be isomorphous with that of $(Al_{4.4}Si_{0.6})(O_{1.0}C_{3.0})$. The separation distance of atoms in the Al3 site was 0.0561(2) nm.

The EDD with $66\times66\times432$ pixels in the unit cell, the spatial resolution of which is approximately 0.005 nm, were obtained from the MPF method using the computer programs RIETAN-FP and PRIMA [16]. After two REMEDY cycles, R_{wp}, S, R_p, R_B and R_F further decreased to 6.94%, 1.22, 5.34%, 1.35% and 0.76%, respectively. Subtle

Table 2
Structural parameters for $Al_5(O_{1.4}C_{2.1}N_{0.5})$.

Site	Wyckoff position	g	x	y	z	$100\times B$ (nm^2)
Al1	4*e*	1	0	0	0.15330(2)	1.22(3)
Al2	4*f*	1	1/3	2/3	0.04474(3)	1.19(3)
Al3	4*f*	1/2	1/3	2/3	0.26299(5)	0.77(4)
(O, C, N)1	2*a*	1	0	0	0	1.76(4)
(O, C, N)2	2*b*	1	0	0	1/4	1.76
(O, C, N)3	4*f*	1	1/3	2/3	0.13325(7)	1.76

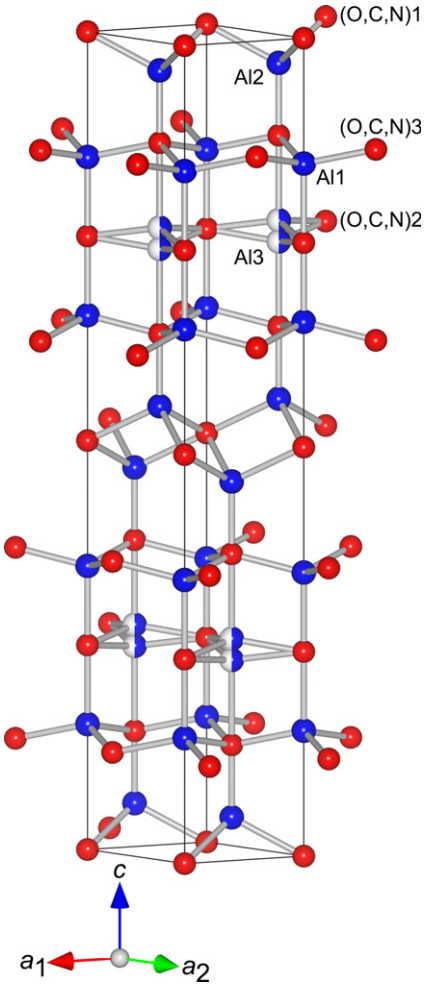

Fig. 4. Crystal structure of $Al_5(O_{1.4}C_{2.1}N_{0.5})$. Space group $P6_3/mmc$. All the atoms are expressed as solid spheres. Because the occupancy of Al3 site is 1/2, the Al atoms occupying there are displayed as blue circle graphs for occupancy. (For interpretation of the references to colour in this figure legend, the reader is referred to the web version of this article.)

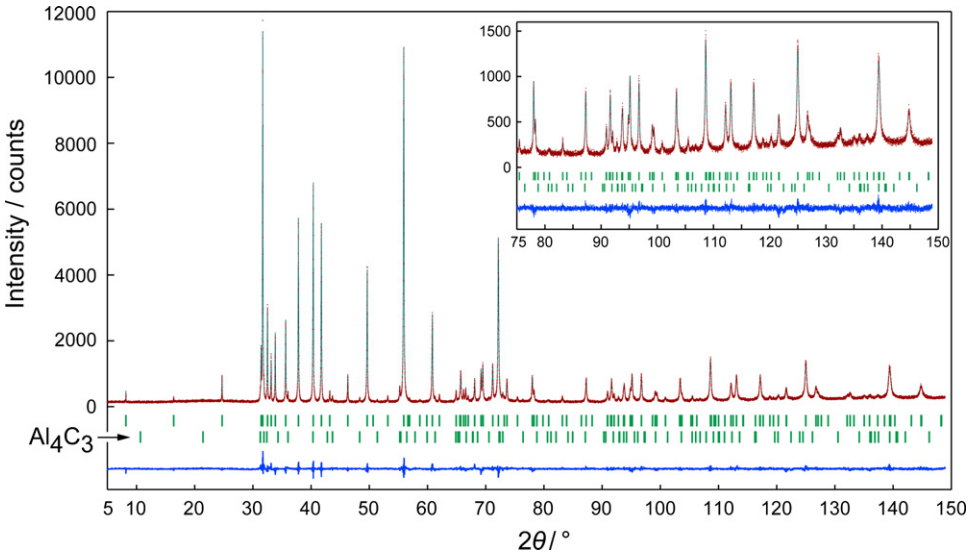

Fig. 5. Comparison of the observed diffraction pattern of $Al_5(O_{1.4}C_{2.1}N_{0.5})$ and Al_4C_3 (symbol: +) with the corresponding calculated pattern (upper solid line). The difference curve is shown in the lower part of the diagram. Vertical bars indicate the positions of Bragg reflections.

EDD changes as revealed by MPF significantly improve the R_B and R_F indices. The decreases in R indices demonstrate that the present disordered structure can be seen more clearly from EDD rather than from the conventional structural parameters reported in Table 2. Observed, calculated, and difference XRPD patterns for the MPF are plotted in Fig. 5. The EDD determined by MPF are in reasonably good agreement with the atom arrangements (Fig. 6). For example, the three-dimensional EDD at the Al3 site was elongated along the *c*-axis, the equidensity isosurfaces of which are in harmony with the atom arrangements. The 2D EDD map at the height of Al3 sites shows that the positions of split Al atoms are successfully disclosed by the EDD (Fig. 7). We found the peak positions of EDD from the 3D pixel data and compared them with the coordinates of all atoms that were determined by the Rietveld method. The positional deviations of all atoms in the unit cell were found to be necessarily less than 0.002 nm, which is within the resolution limit of the 3D EDD. We therefore concluded that, as long as the crystal structure was expressed by a structural model, the present split-atom model would be satisfactory.

3.2. *Description of twinning structure and crystal structure*

In a previous study, the $(Al_{4.4}Si_{0.6})(O_{1.0}C_{3.0})$ crystal has been found to be made up of two domains, which are related by pseudo-symmetry inversion [4]. In a similar manner, the disordered crystal structure of $Al_5(O_{1.4}C_{2.1}N_{0.5})$ can be regarded as a statistical average of the two twin-related structural configurations with the low-symmetry subgroup $P6_3mc$. When the mirror plane perpendicular the *c*-axis is removed from the space group $P6_3/mmc$, the resulting space group is $P6_3mc$, with a center of symmetry being lost concomitantly. The two structural configurations as shown in Fig. 8 are therefore related not only by a pseudo-symmetry mirror plane but also by a pseudo-symmetry inversion. Thus, the crystal must be an inversion twin. Actually we observed using TEM two inter-penetrating domains (Fig. 2). The lattice fringes around the domain boundary showed translational misfit of approximately 0.8 nm along the common *c*-axis.

Each of the two twin-related structural configurations can be regarded as a layered structure, which consists of *A*-type $[Al_4(O, C, N)_4]$ unit layer and *B*-type $[Al(O, C, N)_2]$ single layer. The layer stacking sequences within the unit cell are different between the

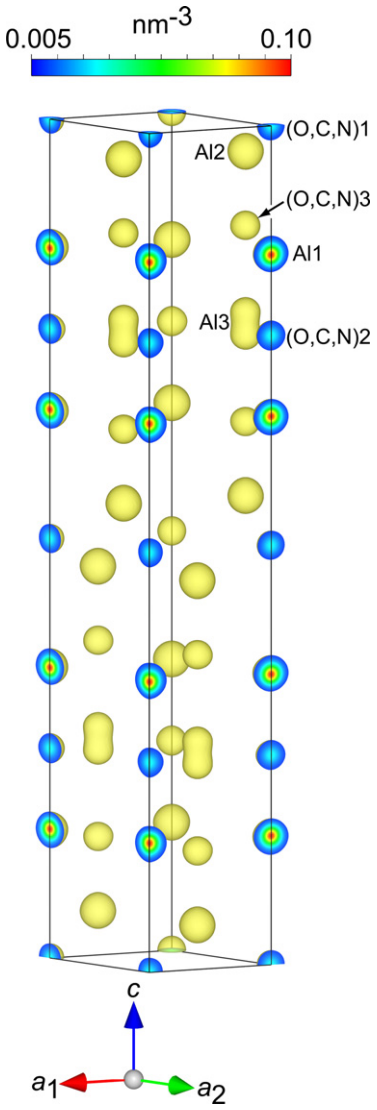

Fig. 6. Three-dimensional electron density distribution determined by MPF. Isosurfaces expressed in smooth shading style for an equidensity level of 0.005 nm^{-3}.

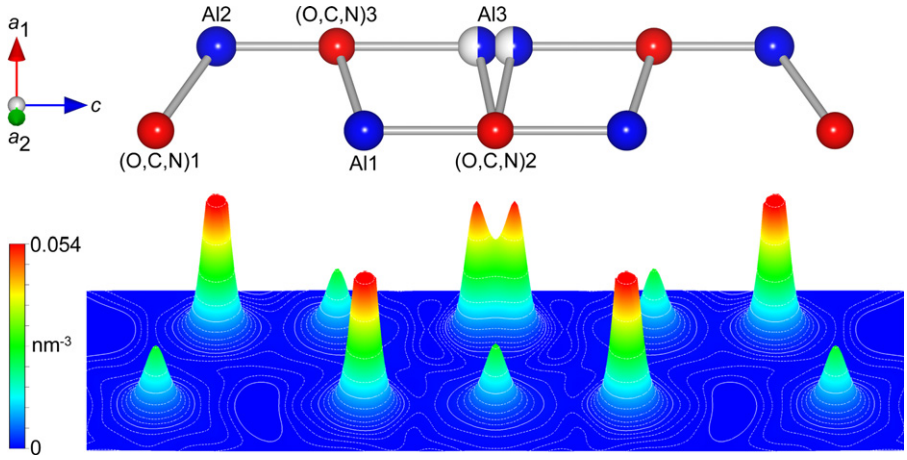

Fig. 7. A bird's eye view of electron densities up to 55.0% of the maximum (0.054 nm^{-3}) on the plane (110) (lower part) with the corresponding atomic arrangements (upper part). Atom numbering corresponds to that given in Table 2.

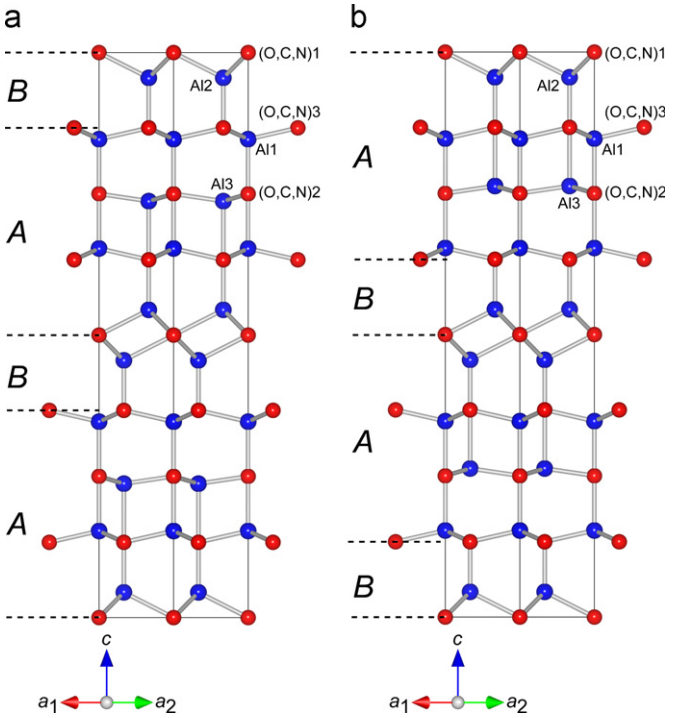

Fig. 8. Crystal structures of the two orientation states of $Al_5(O_{1.4}C_{2.1}N_{0.5})$ viewed along [110], showing the crystal structures being made up of two types of layers *A* and *B*. The two structural configurations (a) and (b) are related by the pseudo-symmetry inversion.

two structures related by a pseudo-symmetry inversion; one is ⟨*ABAB*⟩ along the *c*-axis (Fig. 8(a)) and the other is ⟨*BABA*⟩ (Fig. 8(b)). Thus, the former layer stacking sequence is, with respect to the latter, displaced along the *c* direction by 0.792 nm, which corresponds to the *A*-type layer thickness. These magnitude and direction of displacement are in agreement with those of the misfit between the two interpenetrating domains (Fig. 2). The dimensions of twin domains would be within the coherence range of X-rays and also the domain ratio should be almost 0.5:0.5, hence the crystal structure has been successfully represented by the split-atom model. The present twin boundaries are probably formed during crystal growth or phase transformations. Provided the phase transformation occurred during cooling from 2173 K to ambient temperature, the space group would change from $P6_3/mmc$ of the high temperature phase to $P6_3mc$ of the low temperature phase. The more detailed examination would be necessary for the domain boundaries to determine the origin of the twinning.

Table 3
Interatomic distances (nm) in $Al_5(O_{1.4}C_{2.1}N_{0.5})$.

Al1–(O, C, N)3	0.19451(4) × 3
Al1–(O, C, N)2	0.20887(5)
⟨Al1–(O, C, N)⟩	0.198
Al2–(O, C, N)3	0.19120(3)
Al2–(O, C, N)1	0.21283(3) × 3
⟨Al2–(O, C, N)⟩	0.207
Al3–(O, C, N)2	0.19170(2) × 3
Al3–(O, C, N)3	0.2241(2)
⟨Al3–(O, C, N)⟩	0.200

In Table 3, only Al–(O, C, N) bonds belonging to one of the two twin-related orientations are reported, excluding possible bonds between atoms of different orientation states. The Al atoms are tetrahedrally coordinated by (O, C, N) atoms with the mean Al–(O, C, N) distance of 0.202 nm, which is comparable to the mean (Al, Si)–(O, C, N) distances of the [(Al, Si)(O, C, N)$_4$] polyhedra in $(Al_{4.4}Si_{0.6})(O_{1.0}C_{3.0})$ (0.202 nm) [4] and Al_5C_3N (0.203 nm) [2]. Because the mean interatomic distance as well as the atomic configurations of $Al_5(O_{1.4}C_{2.1}N_{0.5})$ compares well with those of $(Al_{4.4}Si_{0.6})(O_{1.0}C_{3.0})$ and Al_5C_3N, all these compounds can be regarded as, from a structural point of view, a solid solution with the general formula of $(Al_{5-x}Si_x)(O_yC_zN_{4-y-z})$, where *x*- , *y*- and *z*-values are, respectively, 0, 1.4 and 2.1 for the present sample. Further work is necessary to clarify the exact solid solution ranges.

The formation reaction of $Al_5(O_{1.4}C_{2.1}N_{0.5})$ would be accompanied by the oxidation reaction of Al_4C_3 and/or AlN compounds. Actually, the compound Al_4C_3 is unstable at 2173 K near the CCO buffer (Fig. 1). It reacts with CO gas to form Al_2O_3 as follows:

$$Al_4C_3(s)+6CO(g)\rightarrow 2Al_2O_3(s)+9C(s)$$

The by-product graphite is most probably in an amorphous state. On the other hand, the stability of AlN at 2173 K near the CCO buffer is dependent on the partial pressure of N_2 (P_{N_2}). When the P_{N_2} value is less than 0.0072 MPa, which must be the case of the present sample in the furnace, the compound AlN reacts with CO gas to form Al_2O_3 at 2173 K near the CCO buffer (Fig. 1).

Although the thermodynamic behaviors of Al_4C_3 and AlN components in Al_5C_3N might be different from those of the individual compounds Al_4C_3 and AlN, both components would be readily oxidized to introduce oxygen atoms within the crystal structure of Al_5C_3N.

In the system Al–O–C–N, the authors have discovered and structurally characterized a new oxycarbonitride, which has the characteristics of the layered structure. Hence the general formula is expressed by

$$Al_{4l+m}(O, C, N)_{3l+m} \quad (1)$$

where l and m are, respectively, the numbers of A-type $[Al_4(O, C, N)_4]$ unit layer and B-type $[Al(O, C, N)_2]$ single layer of the minimum stacking sequence. The (l, m) values are (1, 1) for $Al_5(O_{1.4}C_{2.1}N_{0.5})$. In a similar manner, new types of oxycarbonitrides are expected to form when O atoms were dissolved into the other ternary carbonitrides than Al_5CN_3. Because the minimum stacking sequences are $\langle BAB \rangle$ for $Al_6C_3N_2$, $\langle BBAB \rangle$ for $Al_7C_3N_3$ and $\langle BBABB \rangle$ for $Al_8C_3N_4$, the corresponding (l, m) values of the general formula (1) are, respectively, (1, 2), (1, 3) and (1, 4).

4. Conclusion

In the Al–O–C–N system, we successfully synthesized a new layered oxycarbonitride $Al_5(O_xC_yN_{4-x-y})$ ($x \sim 1.4$ and $y \sim 2.1$). The crystal structure was satisfactorily represented by the split-atom model, which was isomorphous with that of $(Al_{4.4}Si_{0.6})(O_{1.0}C_{3.0})$, with the space group $P6_3/mmc$ (centrosymmetric). The crystal was composed of the two twin-related individuals with low-symmetry subgroup $P6_3mc$ (noncentrosymmetric), each of which was isostructural with Al_5C_3N.

Acknowledgment

Supported by a Grant-in-Aid for Scientific Research (no. 21360322) from the Japan Society for the Promotion of Science.

Appendix A. Supporting information

Supplementary data associated with this article can be found in the online version at doi:10.1016/j.jssc.2010.08.043.

References

[1] G.A. Jefeerey, V.Y. Wu, Acta Crystallogr. 16 (1963) 559–566.
[2] G.A. Jefeerey, V.Y. Wu, Acta Crystallogr. 20 (1966) 538–547.
[3] T. Iwata, M. Kaga, H. Nakano, K. Fukuda, J. Solid State Chem. 182 (2009) 2252–2260.
[4] M. Kaga, T. Iwata, H. Nakano, K. Fukuda, J. Solid State Chem. 183 (2010) 636–642.
[5] H.M. Rietveld, J. Appl. Crystallogr. 2 (1969) 65–71.
[6] M. Takata, E. Nishibori, M. Sakata, Z. Kristallogr. 216 (2001) 71–86.
[7] F. Izumi, S. Kumazawa, T. Ikeda, W.-Z. Hu, A. Yamamoto, K. Oikawa, Mater. Sci. Forum 378-381 (2001) 59–64.
[8] I.S. Kulikov, Thermodynamics of Oxides, Metallurgiya, Moscow, USSR, 1986.
[9] F. Izumi, K. Momma, Solid State Phenom. 130 (2007) 15–20.
[10] K. Momma, F. Izumi, J. Appl. Crystallogr. 41 (2008) 653–658.
[11] A. Le Bail, H. Duroy, J.L. Fourquet, Mater. Res. Bull. 23 (1988) 447–452.
[12] Th.M. Gesing, W. Jeitschko, Z. Naturforsch. 50b (1995) 196–200.
[13] H. Toraya, J. Appl. Crystallogr. 23 (1990) 485–491.
[14] R.A. Young, in: R.A. Young (Ed.), The Rietveld Method, Oxford University Press, Oxford, UK1993, pp. 1–38.
[15] G.W. Brindley, Bull. Soc. Chim. Fr. (1949) D59–63.
[16] F. Izumi, R.A. Dilanian, in: Recent Research Developments in Physics, vol. 3, Part II, Transworld Research Network, Trivandrum, 2002, pp. 699–726.
[17] M.W. Chase Jr. (Ed.), NIST-JANAF Thermochemical Tables, J. Phys. Chem. Ref. Data Monograph No. 9, 4th ed., American Chemical Society and American Institute of Physics, Woodbury, NY, 1998.